Bulletin of Environment, Pharmacology and Life Sciences
Bull. Env. Pharmacol. Life Sci., Vol 6 [8] July 2017: 112-123

Online ISSN 2277-1808
Journal's URL:http://www.bepls.com
CODEN: BEPLAD
Global Impact Factor 0.533
Universal Impact Factor 0.9804

ORIGINAL ARTICLE **OPEN ACCESS**

Synthesis and Molecular Structure of Mono Nuclear and Binuclear Complexes of Manganese

Manika Barar
Assistant Professor, SIMT College Meerut.

ABSTRACT
3–Methyl–1–phenyl pyrazolone has different biological effects as antipyrine metabolite and is a good biological active molecule. The synthesis and properties of an iron complex [FeCl(TIM)Cl] of the tetraimidazole ligand bis (imidazol–4|–methyl) 4–imidazol–2–yl) methane (TIM) has been reported. Many of these compounds are prepared in attempts to mimic the behaviour of various dicopper proteins such as hemocyanin, tyrosinase etc. Here the present work reports the synthesis and molecular structure of some mononuclear and binuclear manganese(II) complexes with di(μ–OH), (μ–OH) (μ–carboxylato) and tri(μ–carboxylato) groups as bridging ligands.
Keywords : *mononuclear and binuclear manganese(II) complexes, Crystal Data, pharmacological activities.*

Received 10.06.2017 Revised 29.06.2017 Accepted 02.07.2017

INTRODUCTION

Pyrazolone derivatives have been extensively investigated on their wide range of promising pharmacological activities [1, 2]. Hydrazones of pyrazolone derivatives are of current interest due to their high coordinating ability and applications in synthetic and analytical chemistry [3,4] azohydrazone tautomerism of aryl azo derivatives of β–dicarbonyls, naphthols and 2–pyrazolin–5–ones has evoked considerable interest and controversy in the past [5-7]. In addition to the medicinal applications of hydrazones, they have been investigated as donors because of their varied ligational behaviour towards different metal ions and manifestations of novel structural features in the metal complexes [8].

3–Methyl–1–phenyl pyrazolone has different biological effects as antipyrine metabolite and is a good biological active molecule [8-10]. In recent years several other pyrazolone were synthesized such as 4–Acyl pyrazolone [11] but Schiff base pyrazolone has seldom been reported. The reaction of $Mn(ClO_4)_2.4H_2O$ with the ligand normally results in Mn(III) complexes but using electron with drawing substituents on the ligand eg 3–Br or 5–NO_2 gives an Mn(II) complex. In the case of the 5–NO_2–to salen ligand derivative, an Mn(II) complex contaminated with a small amount of Mn(III) species was obtained indicating that this ligand is border line.[12].

The synthesis and properties of an iron complex [FeCl(TIM)Cl] of the tetraimidazole ligand bis (imidazol–4|–methyl) 4–imidazol–2–yl) methane (TIM) has been reported by Mullez et al[13]. Polynuclear metal complexes are of considerable current interest in relation to the nature of magnetic exchange interactions between metal ions through bridging ligands [14-16] and as models for the active sites of metalloenzymes. Many of these compounds are prepared in attempts to mimic the behaviour of various dicopper proteins such as hemocyanin, tyrosinase etc. The active sites of these proteins usually involve copper coordinated to at least two nitrogen donor atoms coming from imidazole of histidine residues. In the (Cu–Zn) superoxide dismutase that the copper ions are coordinated to three imidazoles and one imidazolate (Im^-) group acts as a bridging ligand between the two metals. However it is of interest to note that the structure and chemical composition of the surrounding active site in the metalloproteins [12-18] namely the hydrogen bond network can also modulate their function. Thus the hydrogen bonding between the imidazole moieties and neighboring carboxylate oxygen of the adjacent amino acid residue may orient the ligands for optimal metal coordination and may also enhance the electrostatic interaction between the metal ion and its ligands. Recent studies on the relationship between the junction of enzymes and hydrogen bonding demonstrated that the activity is increased by hydrogen bonding, while it is highly decreased upon hydrogen bonding removal [19, 20].

Manganese Redox Enzymes: There are numerous enzymes that not only have a specific requirement for manganese but also utilize the redox capabilities of this element [21]. Manganese redox enzymes are as follows.

Manganese peroxidase (MnP) is one of the two known enzymes capable of the oxidative degradative degradation of lignin [22]. The MnP is unique in that it absolutely requires Mn(II) to complete its catalytic cycle[23]. The enzyme can be oxidized to an Fe(IV) porphyrin radical by H_2O_2. This radical then reduced twice by Mn(II) giving two free Mn(III) species. Certain α–hydroxy acids promote this reaction through the chelation of Mn(III). In the absence of these acids manganese dioxide is formed. The resulting Mn(III) species then proposed to be responsible for diffusion into the lignin matrix and initiation of phenolic radical decomposition of the polymer.

Manganese thiosulphate oxidase– it has been recently determined that *Thiobacillus versutus* specifically require manganese for the oxidation of thiosulfate to sulfate [24] and appear to be part of a multienzyme system to utilize thiosulphate. EPR evidence seem to indicate a binuclear Mn(II) site and the Mn(II) bound to the S–H group near site is involved in the reaction.

Manganese superoxide dismutase (Mu–SOD) catalyzes the dismutation of superoxide ion (O^{2-}) [25] and protects living cells against the dioxygen dependent toxicities of viologens, quinines, hypervalent compounds and benzofurans [26]. The enzyme is found in mitochondria, chloroplasts and prokaryotes. The Mn–SOD from *Thermus Thermophilus* has been crystallized and X–ray structure [27] shows that it is tetramer. The Mn in Mn–SOD adopts a trigonal–bipyramidal coordination geometry with a N_3O_2 ligand donor set, one histidyl nitrogen occupies the apical position while water is suggested to sit at the opposite site. The carboxylate oxygen from aspartate is bound to the manganese unidentatly, constructing the basal plane with two other histidyl nitrogen atoms. The non liganding oxygen from the aspartate forms a hydrogen bond with an amino acid residue or the peptide backbone. The managanese is believed to cycle between 3^+ and 2^+ oxidation in a ping–pong type mechanism fact supported by the observation that the metal active center does not alter when enzyme is reduced to the Mn(II) ion.

Manganese catalase enzymes are present in most aerobic forms of life and are responsible for the decomposition of hydrogen peroxide to molecular oxygen and water. The Mn catalase has been characterized from new bacteria. The most extremely studied enzymes come from extremely thermophilic *Thermus thermophilus* and lactate requiring *Lactobacillus plantarumn* [28]. The enzymes exists a hexamer of six equivalent subunit, each with a molecular mass of 35 kDa. A 3Å X–ray structure of *Thermus thermophilux* Mn catalase has revealed a four helices bundle motif as the major secondary and tertiary proteins folding element in each unit, each subunit contain a pair of Mn ions separated by 3.6 Å in a reduced state of the enzyme [29]. The manganese catalase enzyme contains a dinuclear center and is believed to cycle between the MnII/MnII and MnIII/MnIII oxidation level during catalysis [30]. Some microorganisms, which are unable to synthesized heme, can nevertheless produce a catalase. This catalase which in contrast to heme–containing catalse is not inhibited by CN^- or N^{3-}, has been called pseudocatalases. Pseudocatalases was first observed in pediococii. It is also called azide–insensitive.

One of the most important reactions occurring in plants is the light driven oxidation of water to oxygen and protons. Most of the oxygen in the atmosphere, which supports acerobic life on earth is generated by plants, algae and cynobacteria by the photoinduced oxidation of water to dioxygen.

$$2H_2O \longrightarrow O_2 + 4e + 4H^+$$

Oxygenic photosynthesis that involves the oxidation of H_2O to O_2 by the Mn–OEC in the chloroplasts, and aerobic respiration that ultimately leads to reduction of O_2 to H_2O by cytochrome c oxidase in the mitochondria together form a cycle of dioxygen metabolism that is critical to both plant and animal life on earth.

Molecular oxygen is relatively abundant in the atmosphere primarily because of its constant regeneration by Mn–OEC catalyzed photosynthetic water oxidation. The conversion of light energy into chemical potential is accomplished very efficiently by photosynthetic organisms. Higher plants, algae and cyanobacteria, in particular, are able to make use of water as an abundant raw material and oxidize it into molecular dioxygen, while producing reduced compounds with a reduction potential equivalent to that of molecular hydrogen.

Photosystem is unique among this group of enzymes in that other transition metals have not been found to function in place of Mn, whereas alternate naturally occurring form of superoxide dismutase and catalase exit which contain Fe instead of Mn. A common structural feature found in most binuclear proteins and enzymes is the presence of one or more bridging (μ) carboxylates derived from aspartate or glutamate side chains of the protein. The bridging carboxylates probably serve a functional role beyond merely that of a passive structural bridge to bring the metal ions together. Their size and negative charge enables them to spatially separate and electrically screen the metal ions so that the degree of

intermetallic electronic coupling is small, $Mn_2^{II, II}$ (μ–carboxylate) [31-33] complexes are relevant examples with weak electronic coupling.

Coordination chemistry of metal carboxylato species is attractive subject from the bioinorganic standpoint because the carboxylate group of glutamate and aspartate works as a supporting ligand for the metal centers in various metalloproteins. The carboxylate groups also suggested to play an important role for structural holding and proton transfer via hydrogen–bonding interaction in proteins. Especially, a bimetallic μ–carboxylato complex is the most attractive synthetic target because the carboxylato–bridged bimetallic core is the common structural motif of the O_2–metabolic non–heme Fe and Mn–proteins such as MMO, RR, Hr(Fe) and catalase (Mn) [34]. Recent advance of X–ray crystallographic works for metalloproteins reveals the variety of the coordination mode of the carboxylate ligands and formation of hydrogen–bonding interaction with the other protic group [35].

Dinuclear Mn complexes containing carboxylato bridges have attracted much attention in recent years because of its potential biological relevance's and several Mn–containing proteins are thought to contain a polynuclear manganese center bridged with carboxylates. It is well established that manganese ions easily polymerize and form dinuclear, trinuclear and higher nuclear complexes in the presence of carboxylates. Accordingly, a variety of polynuclear manganese carboxylato complexes are known [36] and some of them serve as structural analogues for the manganese sites in the oxygen evolving complex of PS II ribonucleotide reductase[37] and manganese catalase [38]. Recently $(\mu\text{–carboxylato})_n$ units, where n = 1–3, were pointed out as a plausible bridging structure of the dimanganese(II) in the manganese substituted ribonucleotide reductase or the fully reduced manganese catalase. Some dinuclear manganese(II) complexes having $(\mu\text{–carboxylato})_{2-4}$ units have been reported [38]. All these complexes, however, adopt a symmetric structure except [39]. Here the present work reports the synthesis and molecular structure of some mononuclear and binuclear manganese(II) complexes with di(μ–OH), (μ–OH) (μ–carboxylato) and tri(μ–carboxylato) groups as bridging ligands.

RESULTS AND DISCUSSION

The hydrotris (3,5–diisopropyl–1–pyrazolyl)borate ($C_{27}H_{46}N_6BK$) (KTp^{iPr2}) has been prepared by the method describe in chapter 2 (Scheme 2.1).

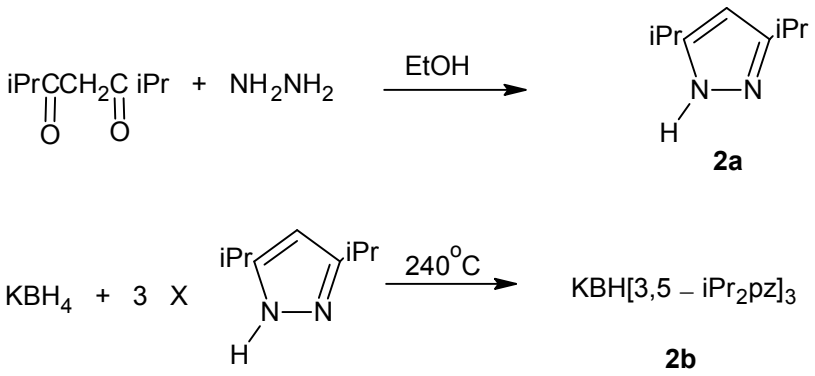

Scheme - 2.1

The synthesis of manganese complexes in +II oxidation state have been tried. The Tp^{iPr2} form LMX type complexes which have very good solubilities in different solvents for further reactions.

The Tp^{iPr2} (Fig. 2–1) has been chosen for present study due to some other excellent properties.

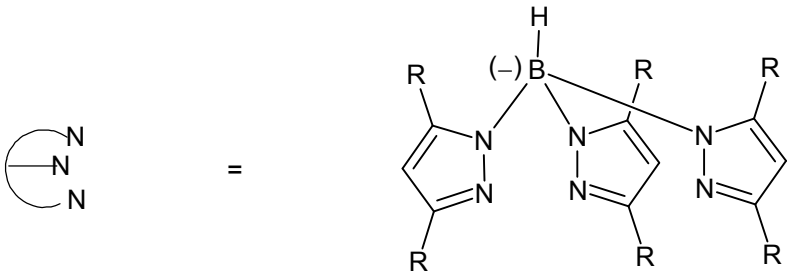

Fig. 2.1

It is:

1. N_3 ligand donor set;
2. Strong electron donor;
3. Highly soluble in CH_2Cl_2, toluene, pentane etc.;
4. Successfully preventing the formation of L_2M;
5. Flexible for variety of coordination geometries.

The reaction of $MnCl_2$ and KTp^{iPr2} gives a mononuclear high spin $Mn(Cl)Tp^{iPr2}$ complex 2c (Scheme 2–2), whose crystal structure is shown in

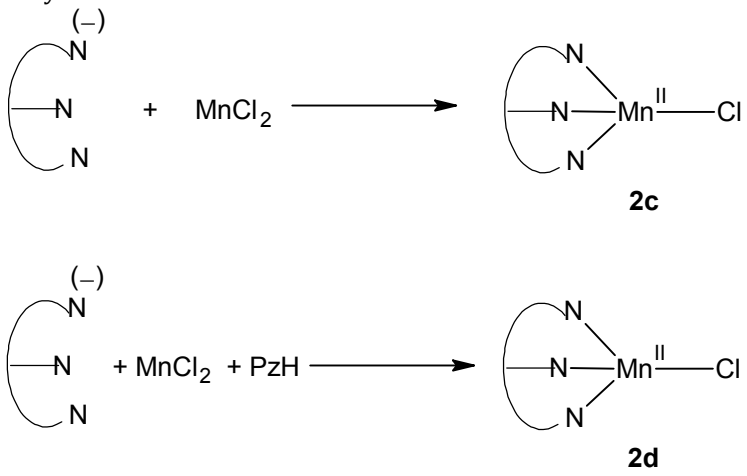

2c

2d

Scheme 2.2

Fig. 2.2. Complex 2c ($C_{27}H_{46}N_6BClMn$) is four coordinate with tetrahedral geometry and Mnl–Cll bond distance 2.272(3) Å. The Mnl–N11, 2.108(8), Mn1–N21, 2.101(7) and Mn1–N31, 2.117(7). On the other hand, the reaction of MnCl2 and KTp^{iPr2} in the presence of 1.5 equivalent amount of free PzH (Pz) (Scheme 2.2) also gives a mononuclear high spin $Mn(Cl)(Pz)Tp^{iPr2}$ 2d ($C_{36}H_{61}N_8BCl$) complex with pyrazole adduct. Its crystal structure is shown in Fig. 2.3. Complex 2d is five coordinate with very distorted geometry with a N_4Cl ligand donor set. Significant disorders are observed for the positions of methyl groups. The Mn1–C11 bond distance is 2.363 Å, which is slightly longer than Mn–Cl bond distance in $[Mn_2Cl_4(O–C_6H_4–p–CH_3)_2]^{-2}$ (2.32 Å) [40] and shorter than Mn–Cl terminal bond distance in LMn_2Cl_2Br (2.491 Å)[40b] but very close to those found for five coordinate [MnTPPCl)]K[(K222)], Mn–Cl bond distance is 2.364 Å[40c]. The distances between manganese and nitrogens of the coordinated ligand are slightly differ from each other (Mn1–N21, 2.151 Å; Mn1–N31, 2.157 Å; Mn1–N41, 2.372 Å) and considerably longer than distance reported for $[Mn(HB(3,5–Me_2pz)_3]^{+2}$ (1.96–1.98 Å)[41] and 2.05–2.23 Å in $[Mn_2O(O_2(CH_3)_2(HB(pz)_3)_2]CH_3CN$[42]. Complex 2c and 2d are stable under air in the solid state and even in solution, it does not react with O_2 and CO_2. Finally, $Mn(Cl)Tp^{iPr2}$ and $Mn(Cl)(Pz)Tp^{iPr2}$ are ideally suited as starting material for the synthesis of other mononuclear and dinuclear complexes by substitution of the chloride ion with other anions. The synthetic utility of the complexes 2c and 2d will be shown in the following studies.

Complex 2e ($C_{54}H_{94}N_{12}O_2B_2Mn_2$) has been prepared by the reaction of $Mn(Cl)Tp^{iPr2}$ with 1N aqueous NaOH in toluene (Scheme 2.3). As shown in Fig. 2–4, it has binuclear structure bridged by two hydroxo groups. The presence of hydroxo groups have been suggested on the basis of ν(OH) band assignment at 3700 cm^{-1}[43]. The molecule is dimeric with each manganese atom binding to two bridging hydroxyl

groups and to three pyrazole nitrogens of the tripod ligand. The Mn–N distances are Mn–N1, 2.270(8), Mn–N2, 2.287(9), Mn–N3, 2.207(8) Å. The short Mn–N3 bond is presumably the result of strain in the N3–Mn–O1 moiety

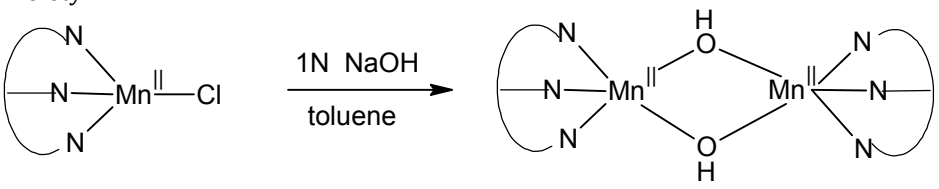

2c **2e**

Scheme 2.3

induced by the binding of the two metal centers in a binuclear fashion with a Mn–Mn separation of only 3.314(8) Å which is very close to Mn–Mn separation in other Mn(II) dimer bridges by phenolate oxygen viz. 3.300 Å in $[Mn(SALPS)]_2$ [44]. 3.256 Å in $[Mn(bpeap)(THF)]_2^{+2}$ [45] and in reasonable agreement with Mn–Mn separation (3.6 Å) of catalase from *Thermus thermophilus.* The Mn–Ol and Mn–O2 bond distances are 2.093(7) and 2.096(8) Å respectively are very close to each other, are in symmetry and are in the range expected for binuclear manganese(II) complexes [46]. The similar structure for di(μ–hydroxo) dimanganese(II, II) is available in literature.

The room temperature magnetic moment is 6.98 B.M./molecule and 4.86 B.M./Mn^{2+} ion (smaller than the spin–only value of 5.92 B.M. for a high–spin d^5 ion).

We have examined the reaction of the Mn(II)–hydroxo precursor with carboxylic acids under various reaction conditions. The anaerobic reaction of 2e ($C_{54}H_{94}N_{12}O_2B_2Mn_2$) with an equimolar amount of benzoic acid in toluene in the presence of anhydrous Na_2SO_4 gave a dinuclear complex 2f ($C_{61}H_{98}N_{12}O_3B_2Mn_2$) (Scheme 2–4). Although we have not yet succeeded in determining the crystal structure, the analytical data. FDMS (field desorption mass spectroscopy) and some other spectroscopic data are all consistent with this structure. Recently the crystal structure of the diferric state of ribonucleotide reductase was reported [47]. The diiron site contains a μ–oxo–μ–carboxylato bridge. The complex 2f ($C_{61}H_{94}N_{12}O_3B_2Mn_2$) thus, may also serve as a structural model for the fully reduced state of Mn–containing ribonucleotide reductase.

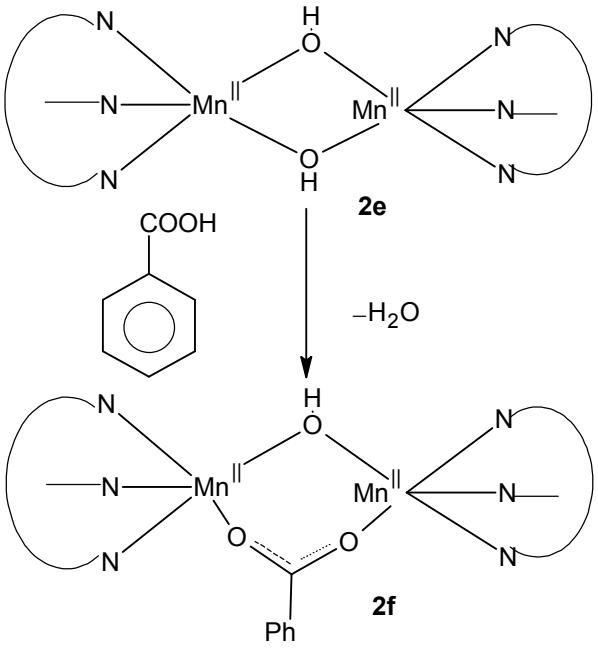

Scheme 2 – 4

In an attempt to replace both hydroxide ligand, the reaction of 2e ($C_{54}H_{94}N_{12}O_2B_2Mn_2$) with excess of benzoic acid in heterogenous system and in the presence of dehydrating agent (anhydrous Na_2SO_4) gave 2g ($C_{75}H_{108}N_{12}O_6B_2Mn_2$) (Scheme 2–5).

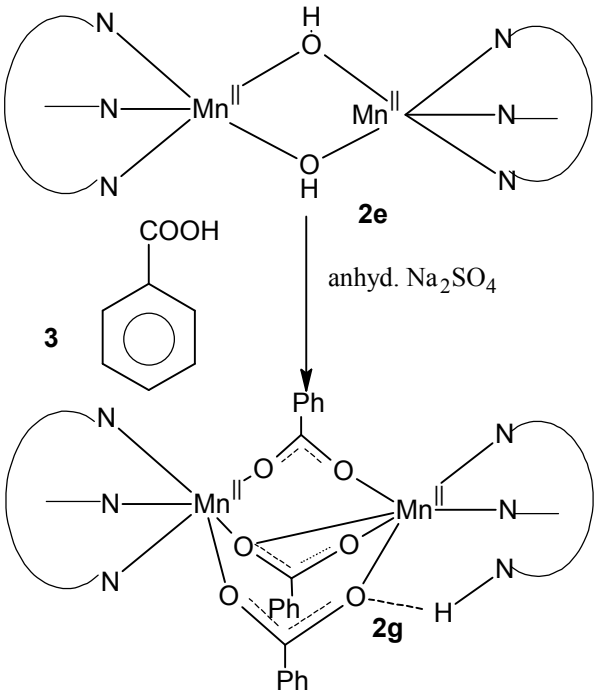

Scheme 2 – 5

use of the aprotic solvent (tolune) prevented the hydrolysis of the B–N bonds of Tp^{iPr2}. We assume that "oxygen donor rich" coordination environment is favorable for hard–acid metal ions and, therefore, oxophilic nature of the manganese makes possible the formation and isolation of the bimetallic tri(μ–carboxylato) complex. In fact, the complex 2g ($C_{75}H_{108}N_{12}O_6B_2Mn_2$) is reasonably air stable even in solution.

The molecular structure of 2g ($C_{75}H_{108}N_{12}O_6B_2Mn_2$) was determined by X–ray crystallography. X–ray crystallography revealed a unique molecular structure of 2g (Fig. 2–5). Dinuclear manganese centers were bridged by three carboxylate ligands, but their coordination environments were extremely different. An octahedral manganese center (Mn1) was supported by an N_3O_3 donor set arising from the normal η^3 binding Tp^{iPr2} ligand and the carboxylate bridges. Whereas another five coordinated manganese (Mn2) was surrounded by N_2O_3 donors coming from three carboxylic oxygen donors and the protonated Tp^{iPr2} ligand ($Tp^{iPr2}H$); a non Mn binding pyrazolyl nitrogen atom (N61) was protonated and the resulting "free acid form" of $Tp^{iPr2}H$ served as a neutral η^2– N, N|–chelating ligand. The structural characterization of the metal binding Tp^RH is extremely rare[48] because protonation causes dissociation from the metal center and, in addition, B–N linkage on Tp^R is readily hydrolyzed under acidic condition. Remarkably, the resulting pyrazolyl N–H group (N61–H1) interacted with a metal binding carboxylic oxygen atom (O92) via hydrogen bonding. The relatively short H1---O92 distance of 1.66(9) Å indicates a strong interaction and that may stabilize the whole structure of 2g. In other words, N61 played as a proton–acceptor during the third carboxylate– bridge formation. Such a ligand exchange process is suggested to be involved in some enzymatic reactions, e.g. binding of protic substrate[49]. Moreover it is widely accepted that the imidazolyl ε–nitrogen of histidine residue works as the proton acceptor in the active site of enzymes.

It is known that carboxylate groups show various coordination mode since the oxygen donor has two lone pairs (i.e. syn and anti pairs) both of which can participate in coordination to the metal center[49]. In fact, the bridging mode of O71–C71–O72 skeleton can be described as anti–syn mode while the other carboxylate bridges had syn–syn mode. Steric repulsion between the isopropyl substituents on the pyrazolyl groups and phenyl group of benzoate resulted in the anti lone pair coordination of O71. The remaining syn lone pair of electrons is directed to Mn2 suggesting the weak interaction, although the O71–Mn2 distance of 2.633(4) Å is out of the range of bonding interaction. In addition, the above mentioned intramolecular hydrogen bonding interaction can also be attributed to the bridging ability of the carboxylic oxygen atom; Mn2–O92 bond is formed through the O92 syn lone pair and the remaining anti lone pair interacts with Hl.

The magnetic susceptibility of the powder sample of 2g ($C_{75}H_{108}N_{12}O_6B_2Mn_2$) is 8.08 B. M./molecule at 295 K, indicative of a weak antiferro–magnetic property.

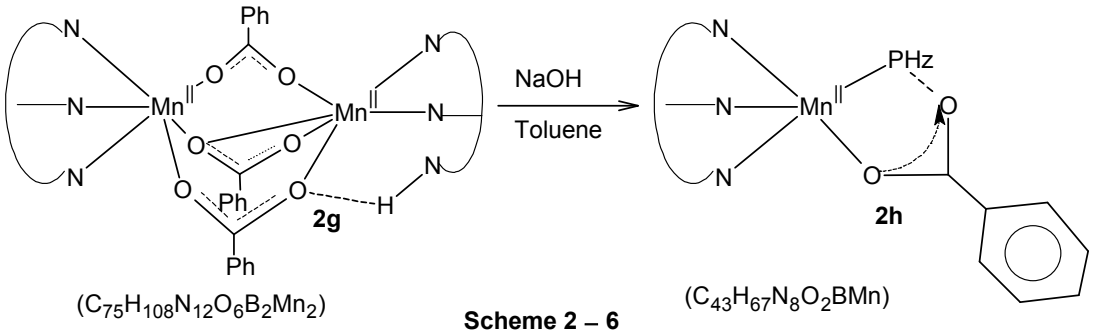

$(C_{75}H_{108}N_{12}O_6B_2Mn_2)$ $(C_{43}H_{67}N_8O_2BMn)$

Scheme 2 – 6

The reaction of 2g with 1 equivalent of NaOH (powder) in toluene (Scheme 2–6) to replace one μ–benzoate gave only a mononuclear manganese(II) complex 2h ($C_{42}H_{67}N_8O_2BMn$). The detailed X–ray structure is given in Fig. 2–6. Complex 2h posseses a monomeric structure with a N_4O ligand donor set. The benzoate groups is coordinated to the manganese unidentately. The non liganding oxygen atom (O_2) of the benzoate forms a hydrogen bond with the proton (Ha) on PzH. The coordination geometry of 2h may be the best describe as distorted trigonal bipyramidal with N2 and N4 as apical ligands. The same compound was prepared by the reaction of 2d ($C_{36}H_{61}N_8BClMn$) with 1.0 equivalent of NaOBz by Kitajima et al. [50]. Thus the structural feature of 2h ($C_{43}H_{67}N_8O_2BMn$) are close to those known for the active site of Mn–SOD [51]. The manganese in Mn–SOD adopts a trigonal–bipyramidal coordination geometry with a N_3O_2 ligand donor set. One histidyl nitrogen occupies the apical position while water is suggested to sit at the opposite site [52]. The carboxylate oxygen from aspartate is bound to the manganese unidentately as in the case of 2h, constructing a basal plane with two other histidyl nitrogen atoms. The nonliganding oxygen from the apartate forms a hydrogen bond with an amino acid residue or the peptide backbone [53-55].

In the ligand spectrum, the bands assigned to pyrazolyl group are present at 1600, 1570, 1483, 1450, 1330, 1070, 1032, 1016, 998, 763, 750 and 682 cm^{-1}, while the bands at 1600, 1500, 1483, 1451 and 1330 cm^{-1} have shifted towards higher wave numbers (~ + 10 cm^{-1}), those at 1071, 1032, 1016, 998, 763, 750 and 682 cm^{-1} have not been shifted and the shift in the positions of the remaining alkyl group bands at lower wave numbers are relatively small and variable (± 5 cm^{-1}). It indicates that possibly the positions of only those bands are shifted which have some contribution from ν(C=C) while the positions of those which have contributions from (C–H) vibrational mode [56] do not change. Another sharp band at 2580 cm^{-1} ν(–N=N–) indicates that pyrazolyl tertiary(57) nitrogen atom coordinated to Mn(II).

Mn(II) complexes are found to be paramagnetic, which are typical of high spin species. Since the analytical data suggest four monodentate ligands around the manganese ion, a tetrahedral geometry of the complex has been assumed. The magnetic moment of Mn(II) complex is 5.75–5.80 B.M. The magnetic moment of both octahedral and tetrahedral Mn(II) complexes should be the same since a 6S–ground state persists in all symmetries. However, the bands at 19500 cm^{-1} and 24000 cm^{-1} which may be assigned to $^4E(G) \leftarrow {}^6A_1$ and $^4A_1(G) \leftarrow {}^6A_1$ transitions respectively are characteristic of four coordinate tetrahedral Mn(II) complexes [58].

SUMMARY

The reaction of hydrotris(3,5–diisopropyl–1–pyrazzolyl)borate (Tp^{iPr2}) with $MnCl_2.4H_2O$ resulted the formation of complex 2c($C_{27}H_{46}N_6BClMn$) and 2d ($C_{36}H_{61}N_8BClMn$) which have vacant coordination site on manganese for important reactivity studies. Complex 2c and 2d are used to prepared complex 2e ($C_{54}H_{94}N_{12}O_2B_2Mn_2$) which upon reaction with one equivalent amount of benzoic acid in toluene gave complex 2f ($C_{61}H_{98}N_{12}O_3B_2Mn_2$) as a possible model compound for the Mn–containing ribonucleotide reductase enzyme.

Reaction of the toluene solution of 2e with solid benzoic acid yielded the complexes 2g ($C_{75}H_{108}N_{12}O_6B_2Mn_2$) contains a unique metallic core structure. The coordination environments (i.e., coordination number and geometry) of the two manganese centers are clearly different. One of the two Tp^{iPr2} ligands, which bound to the five–coordinated Mn center, was protonated by action of the third carboxylic acid and the resulting N–H moiety formed intramolecular hydrogen bond with the oxygen donor of a bridging carboxylate ligand. Steric congestion in the bimetallic core resulted in the large separation of the Mn centers bridged by the syn–anti carboxylate ligand. The above mentioned subjects (i.e., ligand exchange process involving proton transfer, bimetallic core bridged by carboxylates, variation of the coordination mode of the carboxylate) are occasionally observed events in the various metalloproteins and the present results may give some insight into the structural aspects of reaction

intermediates. The reaction of 2g ($C_{75}H_{108}N_{12}O_6B_2Mn_2$) with 1 equivalent solid NaOH gave mononuclear manganese complex 2h Complex 2h ($C_{43}H_{67}N_8O_2BMn$) has distorted trigonal bipyramidal geometry. Further studies on SOD activity of 2h ($C_{43}H_{67}N_8O_2BMn$) and reaction of 2f ($C_{61}H_{98}N_{12}O_3B_2Mn_2$) with different type of nucleotides are in progress.

Table 2.1: Selected Bond Distances (Å) and Angles (deg) for [Mn(Cl)Tp^{iPr2}] (2c) ($C_{27}H_{46}N_6BClMn$)

Interatomic Distances			
Mn1–Cl1	2.272(3)	Mn1–N11	2.108(8)
Mn1–N21	2.101(7)	Mn1–N31	2.117(7)
Bond Angles			
Cl1–Mn1–N11	127.4(2)	Cl1–Mn1 – N21	126.0(2)
Cl1–Mn1–N31	123.7(2)	Nl1–Mn1–N21	88.5(3)
N11–Mn1–N31	90.3(3)	N21–Mn1–N31	89.4(2)
Mn1–N11–N12	115.6(6)	Mn1–N21–N22	116.2(5)
Mn1–N31–N32	115.3(3)		

Table 2.2: Crystal Data and Collection Details of [Mn(Cl)Tp^{iPr2}] (2c)

Emperical Formula	$MnClN_6C_{27}BH_{46}$
Formula Weight	555.90
Crystal System	Monoclinic
Space Group	$P2_1/c$ (≠ 14)
Lattice Parameters	a = 9.937(2) Å b = 16.367(3) Å c = 19.61(1) Å β = 101.007(3)° V = 3130 (2) Å^3
Z value	4
D_{calc}	1.179g/cm^3
Diffractometer	RAXIS–IV
Radiation	Graphite monochromated Mokα (λ=0.71070 Å)
μ(MoKα)/cm^{-1}	5.32
$2\theta_{max}$	55.0°
No. of Measured Reflections	3960
No. Observed Reflections (1 > 3.00 σ(1))	2475
No. of parameters Refined	326
R (based on F)	0.084
Rw	0.084

Table 2.3: Selected Bond Distances (Å) and Angles (deg) for [Mn(Cl)(Pz)Tp^{iPr2}] (2d) ($C_{36}H_{61}N_8BCl.Mn$)

Interatomic Distances			
Mn1–Cl1	2.368(2)	Mn1–N11	2.245(4)
Mn1–N21	2.141(4)	Mn1–N31	2.148(4)
Mn1–N41	2.318(4)		
Bond Angles			
Cl1–Mn1–N11	105.9(1)	Cl1–Mn1 – N21	127.1(1)
Cl1–Mn1–N31	137.2(1)	Cl1–Mn1–N41	88.0(1)
N11–Mn1–N21	81.7(2)	N11–Mn1–N31	80.4(2)
N11–Mn1–N41	166.1(2)	N21–Mn1–N31	95.6(2)
N21–Mn1–N41	90.0(2)	Mn1–N11–N12	114.4(3)
N31–Mn1–N41	89.4(2)	Mn1–N21–N22	116.4(3)
Mn1–N31–N32	116.7(3)	Mn1–N41–N42	115.5(3)

Table 2.4: Crystal Data and Collection Details of [Mn(Cl)Tp^{iPr2}] (2d)

Emperical Formula	$MnClN_6C_{27}BH_{61}$
Formula Weight	706.25
Crystal System	Monoclinic
Space Group	$P2_1/c$ (≠ 14)
Lattice Parameters	a = 13.405(2) Å b = 16.998(5) Å c = 17.544(3) Å β = 92.15(1)° V = 3994.6599 Å^3
Z value	4
D_{calc}	1.177g/cm^3
Diffractometer	RAXIS
Radiation	Graphite monochromated Mokα (λ=0.71070 Å)
μ(MoKα)/cm^{-1}	0.00
$2\theta_{max}$	55.1°
No. of Measured Reflections	6288
No. Observed Reflections (1 > 3.00 σ(1))	3978
No. of parameters Refined	427
R (based on F)	0.058
Rw	0.058

Table 2.5: Bond Distances(Å) & Angles(deg) for [MnTp^{iPr2}]$_2$(OH)$_2$6CH$_2$Cl$_2$ (2e)

Interatomic Distances			
Mn–Mn'	3.314(8)	Mn–O	2.094(4)
Mn–O'	2.089(5)	Mn1–N1	2.270(8)
Mn1–N2	2.207(8)	Mn1–N3	2.287(9)
O–O'	2.553(7)		
Bond Angles			
O–Mn–N1	158.6(3)	O–Mn–N2	114.2(3)
O–Mn–N3	96.2(3)	O–Mn–N1	158.6(3)
O–Mn–N2	114.2(3)	O–Mn–N3	96.2(3)
N1–Mn–N2	87.0(3)	N1–Mn–N3	82.3(3)
N2–Mn–N3	85.9(3)	Mn–O–Mn	104.8(2)

Table 2.6: Crystal Data & Collection Details of [MnTp^{iPr2}]$_2$(OH)$_2$ 6CH$_2$Cl$_2$ (2e)

Empirical Formula	$C_{60}H_{106}N_{12}O_2B_2Cl_{12}Mn$
Formula Weight	1584.51
Crystal System	Monoclinic
Space Group	C2/C
Lattice Parameters	a = 22.132(4) Å b = 13.368(4) Å c = 29.352(7) Å α = 90.00° β = 110.56(3)° γ = 90.00° V = 8131(3) Å
Z value	4
D_{calc}	1.29g/cm^3
Radiation	Graphite monochromated Mokα (λ=0.710680 Å)
μ(MoKα)/cm^{-1}	9.16
$2\theta_{max}$	45.00°
No. of Measured Reflections	5877
No. Observed Reflections	2950
R (based on F)	0.080
Rw	0.077

Table 2.7: Bond Distances (Å) and Angles (deg) for [$Tp^{iPr2}Mn^{II}(\mu–OBz)_3–Mn^{II}Tp^{iPr2}H$] (2g) ($C_{75}H_{108}N_{12}O_6B_2Mn_2$)

Interatomic Distances					
Mn1–N11	2.274(5)	Mn1–N21	2.274(6)	Mn1–N31	2.288(5)
Mn1–071	2.204(4)	Mn1–O81	2.134(4)	Mn1–O91	2.200(4)
Mn2–N41	2.242(5)	Mn2–N51	2.269(5)	Mn2–O72	2.105(4)
Mn2–O82	2.064(5)	Mn2–O92	2.181(4)	Mn2…O71	2.633(4)
N61… O92	2.695(7)	N61–H1	1.190(9)	O92… H1	1.660(9)
Mn1…Mn2	4.006(1)				

Bond Angles			
N11–Mn1–N21	81.5(2)	N11–Mn1–N31	82.7(2)
N11–Mn1–O71	170.5(2)	N11–Mn1–O81	91.7(2)
N11–Mn1–O91	96.5(2)	N21–Mn1–N31	86.4(2)
N21–Mn1–O71	90.0(2)	N21–Mn1–O81	173.1(2)
N21–Mn1–O91	90.8(2)	N31–Mn1–O71	92.7(2)
N31–Mn1–O81	91.5(2)	N31–Mn1–O91	177.2(2)
O71–Mn1–O81	96.8(2)	O71–Mn1–O91	87.6(2)
O81–Mn1–O91	91.2(2)	N41–Mn2–N51	81.5(2)
N41–Mn2–O72	105.1(2)	N41–Mn2–O82	144.1(2)
N41–Mn2–O92	78.5(2)	N51–Mn2–O72	99.9(2)
N51–Mn2–O82	83.4(2)	N51–Mn2–O92	132.2(2)
O72–Mn2–O82	109.5(2)	O72–Mn2–O92	127.0 (2)
O82–Mn2–O92	88.1(2)	Mn1–O71–C71	154.9(4)
Mn2–O72–C71	104.1(4)	Mn1–O81–C81	138.1(4)
Mn2–O82–C81	139.2(4)	Mn1–O91–C91	130.6(4)
Mn2–O92–C91	146.1(4)	N61–H1–O92	141.0(7)
H1–N61–N62	119.0(4)		

Table 2.8: Crystal Data and Collection Details of [$Tp^{iPr2}Mn^{II}(\mu–OBz)_3–Mn^{II}Tp^{iPr2}H$].$2CH_2Cl_2.C_5H_{12}$ (2g)

Emperical Formula	$C_{82}H_{124}N_{12}O_6B_2Cl_4Mn_2$
Formula Weight	1647.27
Space Group	Monoclinic
Crystal System	P 21/n (# 14)
	a = 22.819(3) Å b = 18.226(2) Å c = 22.847(10) Å β = 110.776(4)° V = 8884(4) $Å^3$
Z value	4
D_{calc}	1.231g/cm^3
Diffractometer	RAXIS–IV
Radiation	Graphite monochromated Mokα (λ=0.710680 Å)
μ(MoKα)/cm^{-1}	4.60
$2\theta_{max}$	55.00°
No. of Measured Reflections	12343
No. Observed Reflections (I ≥ 3.0 σ (I)	7590
No. of parameter refined	983
R (based on F)	0.062
Rw	0.060

Table 2.9: Bond Distances (Å) and Angles (deg) for [Mn(OBz)(PzH)Tp^{iPr2}] (2h) ($C_{43}H_{67}N_8O_2BMn$)

Interatomic Distances			
Mn–O1	2.043(4)	Mn–N1	2.195(4)
Mn–N2	2.277(4)	Mn–N3	2.161(3)
Mn–N4	2.304(4)	O2–Ha	1.670(4)
N8–Ha	1.040(4)	C–O1	1.190(8)
C–O2	1.263(7)		
Bond Angles			
O–Mn–N1	153.8(2)	O1–Mn–N2	95.1(2)
O1–Mn–N3	111.3(2)	O1–Mn–N4	92.5(1)
N1–Mn–N2	82.1(1)	N1–Mn–N3	94.3(1)
N1–Mn–N4	89.1(1)	N2–Mn–N3	83.5(1)
N2–Mn–N4	171.2(1)	N3–Mn–N4	97.9(1)

Table 2.10: Crystal Data and Collection Details of [Mn(OBz)(PzH)Tp^{iPr2}] (2h)

Emperical Formula	$C_{43}H_{67}N_8O_2BMn$
Formula Weight	792.75
Crystal System	Triclinic
Space Group	P1
Lattice Parameters	a = 13.635(3) Å b = 16.250(4) Å c = 13.325(4) Å α = 105.72(3)° β = 118.78(2)° γ = 96.41 (2)° V = 2389(1) Å^3
Z value	2
D_{calc}	1.10g/cm^3
Diffractometer	RAXIS–IV
Radiation	Graphite monochromated Mokα (λ=0.710680 Å)
μ(MoKα)/cm^{-1}	3.03
$2\theta_{max}$	50.00°
No. of Measured Reflections	8931
No. Observed Reflections (1 > 3.00σ(1))	4512
R (based on F)	0.053
Rw	0.038

REFERENCES

1. Naik, V.M. & Mathur, N.B., Ind. J. Chem. 41A, 780 (2002).
2. Jain Rajeev, Padma, P., Jyoti Bhaduaria & Tomar Sandeep, J. Ind. Chem. Soc. 77, 42 (2002).
3. Dey, K., Roy, S.B., Bhattacharya, P.K., Gangopadhyay, A., Bhasin, K.K. & Verma, R.D., J. Ind. Chem. Soc. 62, 809 (1985).
4. Sharma, R.C., & Varshney, V.K., J. Inorg. Bio. Chem; 41, 299 (1991).
5. Thankarayan, M. & Nair, M.K., J. Coord. Chem; 53, 1156 (1976).
6. Kousuke Kobashi, Kenji Kurihara & Kazutoyo Hirose, Bull. Chem. Soc. Japan 45, 3551 (1972).
7. Fred, A., Snavely, D.A., & Fay, S.J. & John, I. Farrel, J. Coord. Chem. 10, 1180 (1971).
8. Harode, R. & Sharma, T.C., J. Ind. Chem. Soc. 66, 282 (1989).
9. Kober, Kurtz, G. & Beri, M., Analyt. Chem. 30, 1983 (1958).
10. Mitchel, A. & Nonhebel, D.C., Tetrahedron 35, 2013 (1979).
11. Maurya, R.C. & Verma, R., J. Ind. Chem. Soc. 75, 29 (1998).
12. Mao, L., Rettig, S.J., Thomson, R.C., Trotter, S., Xia, Can. J. Chem. 74, 2413 (1996).
13. Murahashi, S., Oda, Y. and Naota, T., J. Am. Chem. Soc. 114, 7913 (1992).
14. Holm, R.H., Kennepohl, P., Solomon, E.I., Chem. Rev; 96, 2239 (1996).
15. Solomon, E.I., Sundaram, E.U.M., Machonkin, T.E., Chem. Rev. 96, 2563 (1996).
16. Kitajima, N., Morooka, Y., Chem. Rev; 94, 737 (1994).
17. Bertini, I., Bancu L., Luchinat, C., Piccioli, M., Coord. Chem. Rev; 67, 100 (1990).
18. Christianson, D.W., Alexander, R.S., J. Am. Chem. Soc. 111, 6412 (1989).

19. Lesburg, C.A., Christianson, D.W., J. Am. Chem. Soc. 117, 6838 (1995).
20. Kiefer, L.L., Paternos, A., Fierke, C.A., J. Am. Chem. Soc. 117, 6831 (1995).
21. Pecoraro, V.L., Manganese Redox enzymes, VCH, Publishers Inc. New York (1992).
22. Gold, M.H., Wariishi, H., and Valli K., Biocatalysis in agricultural Biotechnology, Chap. 9, Am. Chem. Soc. Washington D.C., 127 (1989).
23. Wariishi, H., Khadar, V. and Gold M.H., Biochemistry 28, 6017 (1989) (b) J. Biol. Chem; 265, 2070 (1990).
24. Cammack, R., Chapman, A., Lu W.P., Karagouni, A., and Kelly D.P., FEBS Lett; 253, 239 (1989).
25. Valentine, J.S. and Motade Freitas D., J. Chem. Educ. 62, 990 (1985).
26. Hassan, H.M. and Fridovich, I., Arch, Bio. Chem. Biophys. 196, 385 (1979) (b) Takahashi, M., Nagano, T., and Hirobe, M., Arch. Biochem. Biophys. 268, 137 (1989) (c) Takabatake, T., Hasegawa, M., Nagano, T. and Hirobe, M., Chem. Pharm. Bull. 39, 1352 (1991) (d) Takabatake, T., Hasegawa, M., Nagano T. and Hirobe, M., J. Biol. Chem. 267, 4613 (1992).
27. Stallings, W.C., Pattridge, K.A., Strong, R.K. and Ludwig, M.L., J. Biol. Chem. 260, 16424 (1985).
28. Kono, Y., and Fridovich, I., J. Biol. Chem; 258, 6015 (1983).
29. Baryn, V.V., Vagin, A.A., Melik, Adamyn V.R., Grebenko, I., Khangulov, S.V., Popov, A.N., Andrianova, M.E. and Vainshtein, B.K., Dolk. Akad. Mauk, SSSR (Crystallogr) 288, 877 (1986).
30. Pennar, Hahn, J.E., In Manganese Redox Enzymes V.L. Pecoraro (Ed) VCH Publishers Inc. New York pp 29 (1992).
31. Guiles R.D., Yachandra, V.K., McDermott, A.E., Cole, J.L., Dexheimer, S.L., Britt, R.D., Sauer, K., and Klein, M.P., Biochemistry 29, 486 (1990). (b) George, G.N., Prince, R.C. and Cramer, S.P., Science 243, 789 (1989) (c) Penner Hahn, J.E., Fronko, R.M., Pecoraro, V.L., Yocum C.F., Bett S.S.D. and Bowlby N.R., J. Am. Chem. Soc. 112, 2549 (1990).
32. Tamura, N., Ikeuchi, M. and Inoue, Y., Biochim. Biophys. Acta 973, 281 (1989).
33. Ghristou, G., Acc. Chem. Res. 22, 328 (1989). (b) Dismukes, G.C., Chem. Rev; 96, pp 2909, 2625 (1996).
34. Lippard, S.J. and Berg, J.M., Chem. Rev; 96, 2237 (1996).
35. Rardin, R.L., Tolman, W.B. and Lippard, S.J., New J. Chem. Chem. 15, 417 (1991).
36. Watkinson, R.G., Garcia, Deibe, M., Bermego M.R. and Sousa, A., J. Chem. Soc. Chem. Commun; 1524 (1992).
37. Willing, A., Follmann, H., and Auling, G., Eur. J. Biochem. 170, 603 (1988).
38. Waldo, G.S. Yu, S. and Penner, Hahn, J.E., J. Am. Chem. Soc. 114, 5869 (1992).
39. Wieghardt, Bossek, U., Nuber, J. Weiss J., Bonovoisn, M., Corbella, M., Vitols, S.E. and Girerd J.J., J. Am. Chem. Soc. 110, 7398 (1988).
40. Cocouvanis, D., Greiwe, K., Salifoglou, A., Challan, P., Simopoulos, A. and Kostikas, A., Inorg. Chem. 27, 594 (1988). (b) Diril, H., Chang, H.R., Zhang, X., Larsen, S.K. Potenza, J.A., Pierpont, C.G., Chang, H.R., Zhang, X., Larsen S.K., Potenza, J.A., Pierpont, C.G., Schugar, H.J., Isied, S.S. and Hendrickson, D.N., J. Am. Chem. Soc; 109, 1425 (1987). (c) Vanatta, R.B., Strouse, C.E., Hanson, L.K. and Valentine, J.S., J. Am. Chem. Soc. 109, 1425 (1987).
41. Chan, M.K. and Armstrong W.H., Inorg. Chem. 28, 3777 (1989).
42. Sheats, J.E., Czernuszewicz R.S., Dismukes, G.C., Rheingold, A.L., Petrouleas, V., Stubbe, J., Armstrong, W.H., Beer, R.H. and Lippard, S.J., J. Am. Chem. Soc. 109, 1435 (1987).
43. Kitajima, N. Fujisawa, K. and Moro, Oka Y., Inorg. Chem. 29, 357 (1990).
44. Kessissoglou, D.P., Butler, W.M. and Pecoraso, V.L., Inorg. Chem. 26, 495 (1987).
45. Hodgson, D.J., Schwartz, B.J. and Sorrel, T.N., Inorg. Chem. 28, 2226 (1989).
46. Shauer, C.K., Anderson, O.P. and Eaton, G.R., Inorg. Chem. 24, 4082 (1985).
47. Nordlund, P., Nature 345, 593 (1990).
48. Kime, Hunt, E., Spartalian K., Derusha, M. Nunn, C.M. and Carrano, B.J. Inorg. Chem. 28, 4392 (1989).
49. Orvile, A.M., Lips Comb. J.D. and Ohlendorf, D.H., Biochemistry 36, 10052 (1997).
50. Kitajima, N. Osawa, M., Tamura N., Moro–oka Y., Hirano T., Hirobe, M. and Nagano, T., Inorg. Chem. 32, 1879 (1993).
51. Parker, M.W., and Blake, C.C.F., J. Mol. Biol. 199, 649 (1988).
52. Shearer, J. & Long, L.M., Inorg. Chem. 45, 2358 (2006).
53. Kramer, R., Angew Chem. 112, 4641 (2000)
54. Aston K., Rath, A., Naik, U., Slomczynska O.F., & Riley, S.P., Inorg. Chem. 40, 1779 (2001).
55. Lui, G.F., Filpovic, M., Heinmannm, F.W. & Burmazovic, II, Inorg. Chem. 46, 8825 (2007).
56. Mohapatra, S.C., Tehlan, S., Hundal, M.S. & Mathur, P., Inorg. Chim. Acta 361, 1897 (2008).
57. Singla, M., & Mathur, P., Spectrochim. Acta (A) 74, 536 (2009).
58. Ali, S.M., Iftikhar, K. & Ahmad N., Synth. React. Inorg. Met. Org. Chem. 13, 699 (1983); 14, 1031 (1984).

CITATION OF THIS ARTICLE

Manika Barar. Synthesis and Molecular Structure of Mono Nuclear and Binuclear Complexes of Manganese. Bull. Env. Pharmacol. Life Sci., Vol 6 [8] July 2017: 112-123